Geoneutrino Fluxes From A Laterally Heterogeneous Lower Mantle: Constraints From Geophysics And Geochemistry

Ondřej Šrámek[1], William F. McDonough[1], Stephen T. Dye[2,3] and Shijie Zhong[4] **U41A-0004**

1 University of Maryland, Department of Geology; 2 Hawaii Pacific University; 3 University of Hawaii; 4 University of Colorado at Boulder, Department of Physics

sramek@umd.edu ; anquetil.colorado.edu/~sramek

1. Summary

- Knowledge of the amount and spatial distribution of heat producing elements (HPEs) in the Earth's interior is crucial for understanding Earth's energetics.
- Compositional estimates for the average silicate (non-metallic) part of Earth's interior show a variability of up to a factor of 3.
- Recent advances in experimental neutrino physics led to detection of **geoneutrinos**, electron-anti-neutrinos emitted in naturally occurring radionuclides' decay chains, which provide a **direct measurement of Earth's internal radioactivity**.
- We present a new analysis of predicted geoneutrino signal from the Earth's mantle for several established compositional estimates of Earth's geochemical reservoirs.
- We illustrate the surface variation of mantle geoneutrino flux using simple conceptual models of the deep mantle structure as well as a seismic tomography-based picture or Earth's interior.
- We relate the flux predictions to existing geoneutrino detections and proposed future geoneutrino experiment sites.

2. Geoneutrino flux calculations

Decay chains of naturally occurring radionuclides ^{238}U, ^{235}U, ^{232}Th and ^{40}K produce electron anti-neutrinos ($\bar{\nu}_e$) and heat Earth's interior:

$$\begin{aligned}
^{238}\mathrm{U} &\longrightarrow {}^{206}\mathrm{Pb} + 8\alpha + 6e^- + 6\bar{\nu}_e + 51.7\,\mathrm{MeV}\\
^{235}\mathrm{U} &\longrightarrow {}^{207}\mathrm{Pb} + 7\alpha + 4e^- + 4\bar{\nu}_e + 46.4\,\mathrm{MeV}\\
^{232}\mathrm{Th} &\longrightarrow {}^{208}\mathrm{Pb} + 6\alpha + 4e^- + 4\bar{\nu}_e + 42.7\,\mathrm{MeV}\\
^{40}\mathrm{K} &\xrightarrow{89.28\%} {}^{40}\mathrm{Ca} + e^- + \bar{\nu}_e + 1.311\,\mathrm{MeV}\\
^{40}\mathrm{K} + e^- &\xrightarrow{10.72\%} {}^{40}\mathrm{Ar} + \nu_e + 1.505\,\mathrm{MeV}
\end{aligned} \tag{1}$$

The anti-neutrino flux $\Phi_X(\mathbf{r})$ at position $\mathbf{r}$ from a radionuclide X distributed in a spatial domain Ω is calculated from [e.g., 1]:

$$\Phi_X(\mathbf{r}) = \frac{n_X \lambda_X \langle P \rangle}{4\pi} \int_\Omega \frac{a_X(\mathbf{r}')\rho(\mathbf{r}')}{|\mathbf{r}-\mathbf{r}'|^2}\mathrm{d}\mathbf{r}' \tag{2}$$

- n_X is the number of anti-neutrinos per decay chain
- λ_X is the decay constant (1/lifetime)
- a_X is the abundance of radioactive isotope (# rad. isotope atoms per kg of rock)
- ρ is rock density
- $\langle P \rangle$ is the average survival probability; assumes a signal source region size much larger than the neutrino oscillation length (60–110 km depending on anti-neutrino energy)

$$a_X = \frac{A_X X_X}{M_X}, \tag{3}$$

- A_X is the elemental abundance (kg of element per kg of rock)
- X_X is the isotopic ratio (atoms of radionuclide per atoms of element)
- M_X is atomic mass

Estimates of HPE abundances and spatial distribution in Earth's interior $\longrightarrow$ calculate the predicted geo-$\bar{\nu}_e$ flux at the surface

3. Geoneutrino detection

Some of the geoneutrinos (from ^{238}U and ^{232}Th) are now detectable.

- 2 experiments reported measurements – KamLAND in Japan and Borexino in Italy
- SNO+ in Ontario, Canada will go on-line in 2012
- proposed detectors – LENA (Finland or France), HanoHano (Hawaii)

Predictions of geoneutrino signal for various compositional estimates can be compared to measurements. Ultimate goal is to experimentally constrain the abundance/distribution of HPEs in Earth's interior.

4. Composition estimates, mass balance

Geochemical reservoirs: BSE = bulk silicate Earth; CC = bulk continental crust; BM = bulk mantle; DM = depleted MORB mantle; EM = enriched mantle

Composition estimates of Earth's geochemical reservoirs

	BSE			CC	DM		
	J et al	A et al	T&S	R&G	W&H	S&S	A&McD
A_U in ppb	12	20	31	1300	3.2	4.7	8
A_{Th} in ppb	42.7	80	124	5600	7.9	13.7	22
A_K in ppm	129	276	310	17000†	50	60	152
Th/U	3.6	4	4.0	4.3	2.5	2.9	2.8
K/U	10750	13800	10000	13000†	15600	12800	19000
Power in TW	**11.0**	**20.2**	**29.6**	7.2	2.8*	4.1*	7.5*

BSE heat production and surface heat flux

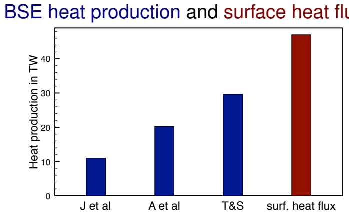

- J et al = Javoy et al. [2] — E-chondrite based
- A et al = Arevalo et al. [3] — CI-chondrite based, modified from McDonough and Sun [4]
- T&S = Turcotte and Schubert [5] — based on energetics of mantle convection
- R&G = Rudnick and Gao [6]; we assume crustal composition to be relatively well-known
- W&H = Workman and Hart [7]
- S&S = Salters and Stracke [8]
- A&McD = Arevalo Jr. and McDonough [9]

Bulk mantle composition from:

" BSE = CC + BM "

Geochemistry usually requires an enriched, possibly "hidden", deep-mantle reservoir:

" BM = DM + EM " or **" BSE = CC + DM + EM "**

Trade-off between the size (mass fraction F^{EM} of the total mantle) of enriched reservoir and the enrichment factor E (EM/DM composition ratio):

$$A_X^{BM} = A_X^{DM}[1 + (E_X - 1)F^{EM}]. \tag{4}$$

5. Cartoon models of HPE distribution, calculated flux

Schematic representation of ULVZ, LLSVPs (piles/superplumes)

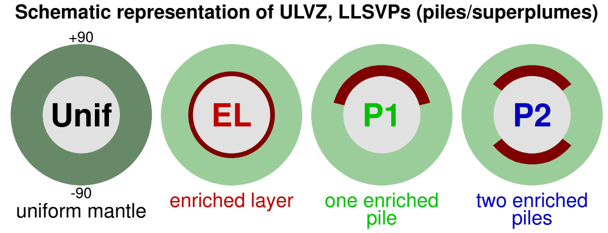

10% is EM, 90% is DM
EM is a 427km-thick layer (EL), or 1000km-thick piles (P1, P2)

Spherically symmetric cases (Unif, EL): geo-$\bar{\nu}_e$ flux variation within a given BSE model

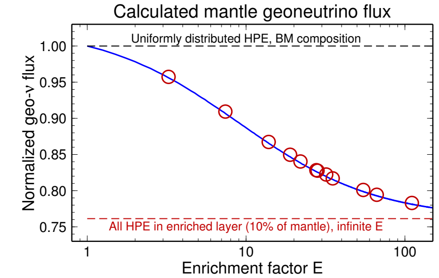

- Maximum flux reduction by 25% when all HPEs concentrated near CMB

Geo-$\bar{\nu}_e$ flux for axially symmetric cases (P1, P2)

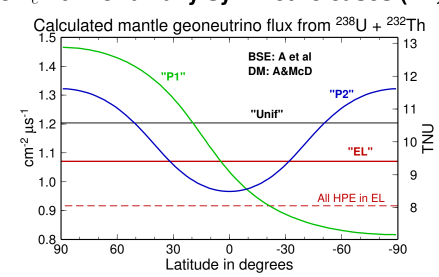

- Surface average value for P1 and P2 identical to case EL
- P1: variation of 49%; P2: variation of 27%

6. Flux for seismic tomo-based enriched reservoir geometry

S20RTS shear-wave speed anomaly [10]

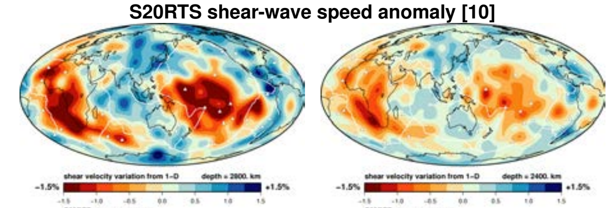

Consider: slow V_S ($< -0.25\%$ below 1500 km) $\Rightarrow$ enriched material

Calculated mantle geoneutrino flux from ^{238}U + ^{232}Th

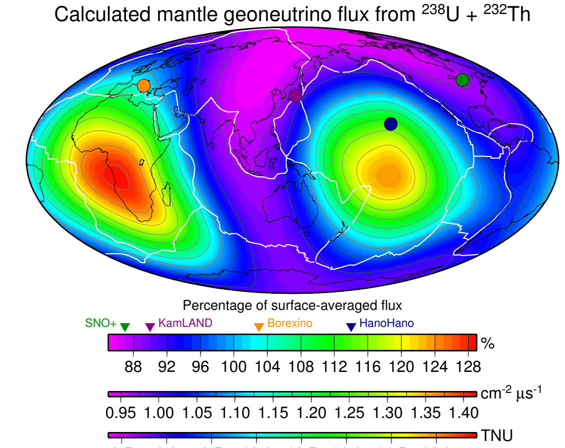

- surface-averaged flux very close to case EL
- 43% flux variation
- 2 flux maxima related to the African and Pacific deep mantle piles

7. Compositional models vs. existing measurements

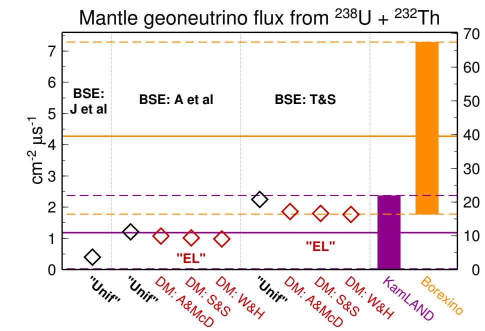

- KamLAND measurement consistent with all 3 BSE composition estimates.
- Borexino measurement only supports T&S BSE (at 1σ level)

Calculated crustal geoneutrino flux from ^{238}U + ^{232}Th [11]

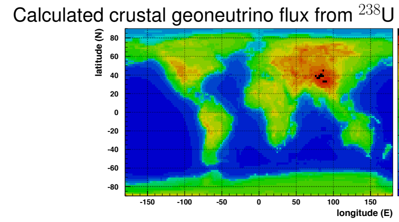

- strong crustal signal at KamLAND, Borexino, SNO+, LENA

8. Conclusions

- Geochemistry (composition estimates) + geophysics (constraints on mantle structure) + experimental particle physics (geoneutrino measurements) $\rightarrow$ toward better knowledge of Earth's radiogenic heat.
- In order to discriminate between different BSE compositional models, we need to measure mantle geoneutrinos with $\lesssim 20\%$ uncertainty.
- This has not been accomplished to date, but improved statistics at operational detectors and future experiments may achieve this goal.
- An oceanic-site detector is highly desirable.

References

[1] Fiorentini, G., M. Lissia, and F. Mantovani, Geo-neutrinos and earth's interior, *Phys. Rep.*, **453**(5-6):117–172, 2007, doi: 10.1016/j.physrep.2007.09.001.

[2] Javoy, M., et al., The chemical composition of the Earth: Enstatite chondrite models, *Earth Planet. Sci. Lett.*, **293**(3-4):259–268, 2010, doi:10.1016/j.epsl.2010.02.033.

[3] Arevalo, R., Jr., W. F. McDonough, and M. Luong, The K/U ratio of the silicate Earth: Insights into mantle composition, structure and thermal evolution, *Earth Planet. Sci. Lett.*, **278**(3-4):361–369, 2009, doi:10.1016/j.epsl.2008.12.023.

[4] McDonough, W. F. and S. Sun, The composition of the Earth, *Chem. Geol.*, **120**(3-4):223–253, 1995, doi:10.1016/0009-2541(94)00140-4.

[5] Turcotte, D. L. and G. Schubert, *Geodynamics, Applications of Continuum Physics to Geological Problems*, Cambridge University Press, second edition, 2002.

[6] Rudnick, R. L. and S. Gao, Composition of the continental crust, in H. D. Holland and K. K. Turekian, editors, *The Crust*, volume 3 of *Treatise on Geochemistry*, chapter 3.01, pages 1–64, Elsevier Scientific Publishing Company, Oxford, 2003, doi:10.1016/B0-08-043751-6/03016-4.

[7] Workman, R. K. and S. R. Hart, Major and trace element composition of the depleted MORB mantle (DMM), *Earth Planet. Sci. Lett.*, **231**(1-2):53–72, 2005, doi:10.1016/j.epsl.2004.12.005.

[8] Salters, V. J. M. and A. Stracke, Composition of the depleted mantle, *Geochem. Geophys. Geosyst.*, **5**(5):Q05B07, 2004, doi: 10.1029/2003GC000597.

[9] Arevalo Jr., R. and W. F. McDonough, Chemical variations and regional diversity observed in MORB, *Chem. Geol.*, **271**(1-2):70–85, 2010, doi:10.1016/j.chemgeo.2009.12.013.

[10] Ritsema, J., H. J. van Heijst, and J. H. Woodhouse, Complex shear wave velocity structure imaged beneath Africa and Iceland, *Science*, **286**(5446):1925–1928, 1999, doi:10.1126/science.286.5446.1925.

[11] Dye, S. T., 2011, personal communication.

2011 AGU Fall Meeting, 5–9 December, Moscone Convention Center, San Francisco, California, USA